

Performance improvement of micro-fuel cell by manipulating the charged diffuse layer

Isaac B. Sprague and Prashanta Dutta

Citation: *Appl. Phys. Lett.* **101**, 113903 (2012); doi: 10.1063/1.4752459

View online: <http://dx.doi.org/10.1063/1.4752459>

View Table of Contents: <http://apl.aip.org/resource/1/APPLAB/v101/i11>

Published by the [American Institute of Physics](#).

Related Articles

Surface-tension driven self-assembly of microchips on hydrophobic receptor sites with water using forced wetting
Appl. Phys. Lett. **101**, 114105 (2012)

Fast acoustic tweezers for the two-dimensional manipulation of individual particles in microfluidic channels
Appl. Phys. Lett. **101**, 114103 (2012)

Uniform and refreshable liquid electroluminescent device with a back side reservoir
APL: Org. Electron. Photonics **5**, 208 (2012)

Uniform and refreshable liquid electroluminescent device with a back side reservoir
Appl. Phys. Lett. **101**, 113302 (2012)

Frequency and Q factor control of nanomechanical resonators
Appl. Phys. Lett. **101**, 103110 (2012)

Additional information on *Appl. Phys. Lett.*

Journal Homepage: <http://apl.aip.org/>

Journal Information: http://apl.aip.org/about/about_the_journal

Top downloads: http://apl.aip.org/features/most_downloaded

Information for Authors: <http://apl.aip.org/authors>

ADVERTISEMENT



HAVE YOU HEARD?

Employers hiring scientists
and engineers trust
physicstoday JOBS



<http://careers.physicstoday.org/post.cfm>

Performance improvement of micro-fuel cell by manipulating the charged diffuse layer

Isaac B. Sprague and Prashanta Dutta^{a)}

School of Mechanical and Materials Engineering, Washington State University, Pullman, Washington 99164-2920, USA

(Received 3 July 2012; accepted 30 August 2012; published online 12 September 2012)

A fuel cell device is presented based on a counter-flow microfluidic fuel cell (CFMFC) with nano-porous electrodes by developing an advection flux of ions within the electric double layer (EDL). Typically, in a microfluidic fuel cell, advection in the EDL is negligible because the near wall electrolyte velocity is zero. However, by using nano-pores, a non-negligible ion flux due to advection can be developed in the charged regions of the EDL which affects the structure of the EDL. In this article, we use a mathematical model to study how advection in the EDL affects the kinetic performance of fuel cells. Our model predicts that the peak power density can be increased by more than 2 fold in a CFMFC using this approach to kinetic enhancement. © 2012 American Institute of Physics. [<http://dx.doi.org/10.1063/1.4752459>]

Recently, there have been several studies investigating how the electric double layer (EDL) affects electrode kinetics¹⁻³ in galvanic cells and how device performance might be improved through the electrolyte.^{4,5} As microfabrication and nano-patterning techniques improve, new possibilities for improving the effective electrode performance are available through electrode microstructure design with features down to the order of the EDL width. Cylindrical electrodes with diameters down to the nano-scale are found to greatly alter electrode kinetics.⁶ The EDL structure has been found to be altered through the use of blind nano-pores in a planar electrode,⁷ and fabrication of nanoporous electrodes on gold and other oxide surfaces are reported recently.⁸ Moreover, nano-scale pores have been used to form ion depletion or enrichment of electrolytes, known as concentration polarization⁹ which impacts ionic currents in electrochemical cells.^{10,11}

Here we introduce an electrode design with nano-scale features to improve performance of laminar flow fuel cell. This is accomplished by flowing an electrolyte and reactant mixture through nano-pores in the electrode, providing an advection flux in regions of nonzero charge density. We present a CFMFC similar to Salloum and Posner¹² where fuel and oxidant reactant streams are fed through opposing porous electrodes before they are diverted to different outlets. However, in this work, we consider a nano-porous electrode with regular pore spacing and structure. This allows for increased performance from better reactant transport, seen at the macro-scale,¹² as well as a more significant performance benefit from nano-scale electrode effects. The experiments are performed numerically to better understand the role of the physics of the advection flux within the EDL.

The device is configured in such a way that the fuel and oxidant inlets are on opposing sides of a planar microchannel. The fuel and oxidant electrolyte streams flow (with an average velocity of V_{Avg}) in a counter flow fashion from their

corresponding upstream inlets through the porous anode and cathode electrodes, respectively, before being diverted to their respective outlets. The two streams are in contact in the middle of the device allowing the conduction of ionic current across the electrolyte, as shown in Figure 1.

For the bulk electrolyte advection through the pores to influence the electrode performance, the physical values of the pore width (d_5) must be on the order of the Debye length ($\lambda_D = \text{width of EDL} \approx 2-20 \text{ nm}$). The intended order of magnitudes of the remaining dimensions are summarized in Table I.

To maintain simplicity in this investigation, we consider a simple acidic binary electrolyte consisting of a cation (C^+) and an anion (A^-) of unit charge, $z_{C^+} = -z_{A^-} = 1$. Additionally, since the electrolyte is acidic, the cation is the working

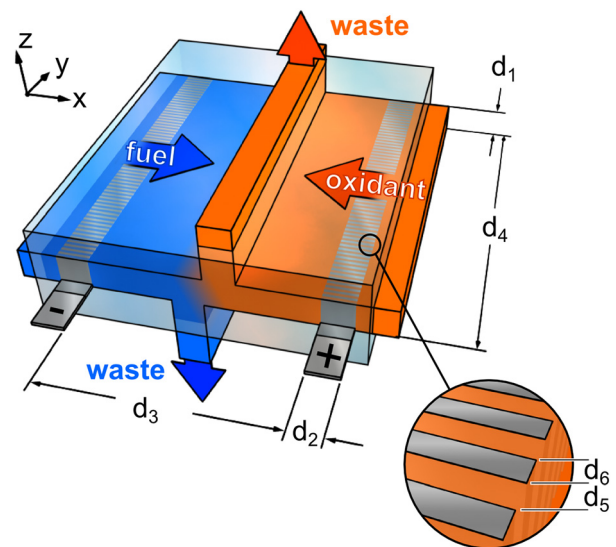


FIG. 1. Device configuration used for electrolyte advection through nano-porous electrodes. The device comprised of two inlets on opposing sides of a microchannel that feed to porous electrodes which are separated by a central region. The nano-pores (inset) are considered to be slots extending the full height of the planar channel.

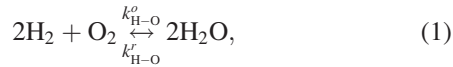
^{a)} Author to whom correspondence should be addressed. Electronic mail: prashanta@wsu.edu. Tel.: (509) 335-7989. Fax: (509) 335-4662.

TABLE I. Intended order of magnitude for key dimensions in porous electrode device.

d_1	10 μm
d_2	1–2 μm
d_3	100 μm
d_4	1 cm
d_5	2–20 nm
d_6	2–20 nm

ion, being produced by fuel oxidation and consumed by oxidant reduction. The anion is inert and does not participate in the electrode reactions. The device configuration is a multi-dimensional domain with very disparate length scales and direct solution of the full domain would not be possible. Results were obtained by dividing the domain into three, 2-dimensional regions in a way that is analogous to domain decomposition techniques used to achieve analytic approximations through asymptotic analysis.¹³ Each region is simulated numerically by solving the Poisson-Nernst-Planck equations as well as the Navier-Stokes equations using custom in-house software, the details of which are presented elsewhere.²

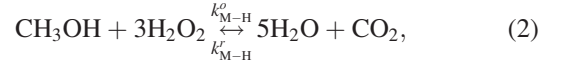
In this work, we consider two systems: a hydrogen and oxygen as well as a methanol and hydrogen peroxide fuel cell. Hydrogen and oxygen (H-O) are considered for the fuel and oxidant using the following stoichiometric reaction:



where k^o and k^r are the oxidation and reduction rate constants, respectively.

However, a H-O micro-fuel cell, with its low maximum reactant concentrations, can be severely transport limited. This is due to solubility limits and because the device operates using reactant streams mixed with a liquid electrolyte. The maximum concentration of hydrogen and oxygen in the electrolyte are around 10 mM and 2 mM, respectively. These low reactant concentrations are easily depleted by the electrode reactions. This can lead to severely reduced electrode reaction rates for downstream regions of the electrodes as the reactions are starved for reactants, which is known as transport limitations. The proposed device design should mitigate these limitations to some degree by passing the

reactant-electrolyte streams through the porous electrodes. To study the device performance in the absence of transport limitations, a second fuel-oxidant combination is also considered, methanol-hydrogen peroxide (M-H), using the following stoichiometric reaction:



while the reaction rate of methanol oxidation and hydrogen peroxide reduction are less than that of hydrogen oxidation and oxygen reduction, their concentrations achievable in a liquid electrolyte mixture are much greater.

The power density performance data for a H-O and M-H device with nano-pore widths that are equal to that of the Debye length ($d_5 = \lambda_D$) are shown in Figures 2(a) and 2(b), respectively. The performance of both the H-O and M-H fuel cells are strong functions of electrolyte flow rate; the peak power is nearly double for a device with $V_{\text{Avg}} = 20$ mm/s than for a device with $V_{\text{Avg}} = 2$ mm/s. This performance improvement is the result of the introduction of an advection flux in the EDL where the electrolyte has a net nonzero charge density. Typically, since the EDL is a near wall phenomenon, there is no advection present because the near wall velocity is zero. However, by flowing the electrolyte through a nano-pore whose width is on the order of the EDL width, the near wall velocity is nonzero and an advection flux acts on the charged regions of the electrolyte.

The presence of this advection flux alters the balance between the diffusion and migration fluxes within the EDL, causing the distribution of positive and negative ions to shift. This change in EDL structure along the nano-porous electrode yields a higher total electrode current for an equivalent potential. As shown in Figure 2, the greater the electrolyte velocity, the greater the increase in electrode power density because of a greater change in the EDL structure. It was found that the shift in ion concentration distributions is reducing the electrostatic restriction on kinetics and allows them to proceed at or near their spontaneous thermodynamic rates (not shown). These results suggest that a device capitalizing on this EDL advection effect, such as the nano-porous counter flow device presented here, could yield significantly greater performance with device efficiencies much closer to the thermodynamic maximum.

It is also important to note that the performance of the M-H device is better than the H-O device for all flow rates

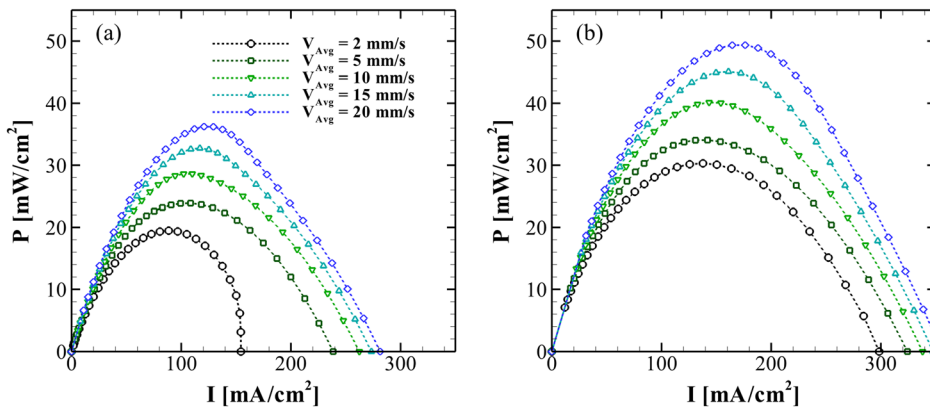


FIG. 2. Power density performance for a (a) H-O and (b) M-H device with nano-pore widths are equal to that of the Debye length ($d_5 = \lambda_D$) and various average electrolyte velocities, V_{Avg} . The average electrolyte velocities used are: 2, 5, 10, 15, and 20 mm/s. ($d_2 = 1 \mu\text{m}$, $k_{\text{H-O}}^o = 5 \times 10^{-6}$ m/s, $k_{\text{H-O}}^r = 5 \times 10^{-7}$ mol/m²s, $k_{\text{M-H}}^o = 5 \times 10^{-8}$ m/s, $k_{\text{M-H}}^r = 1 \times 10^{-9}$ mol/m²s).

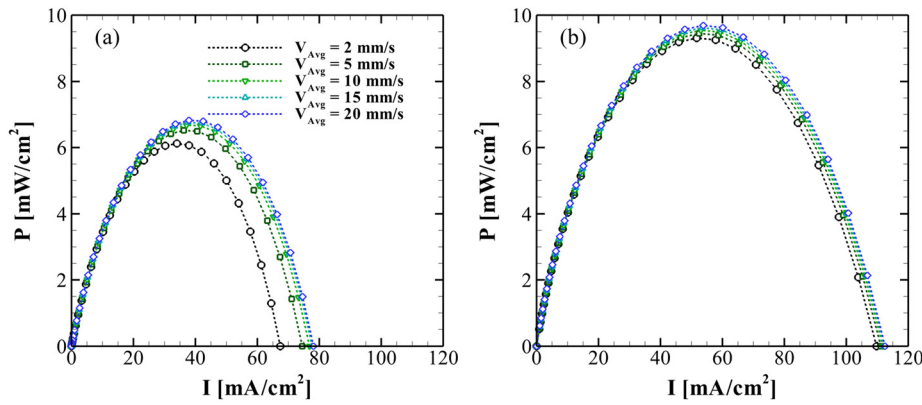


FIG. 3. Power density performance for a (a) H-O and (b) M-H device with nano-pore widths 10 times that of the Debye length ($d_5 = 10\lambda_D$) at various average electrolyte velocities, V_{Avg} . All other conditions are the same as in Figure 2.

despite slower kinetic rates. In fact, in this study, we took the M-H rates to be slower by factors of 100 and 500, respectively, but only increased the inlet concentrations by factors of 50 and 250. Consequently, the H-O device would outperform the M-H device in the absence of reactant transport limitations. Clearly, transport limitations through a nano-pore are not easily overcome in the range of flow rates studied. This suggests that this device architecture, as is common with many micro-fuel cells, is better suited for liquid reactants.

The power density performance data for a H-O and M-H device where the nano-pore widths are 10 times that of the Debye length ($d_5 = 10\lambda_D$) are shown in Figures 3(a) and 3(b), respectively. It can be seen that the performance of both the H-O and M-H fuel cells is no longer a significant function of flow rate. Although, the H-O device performance does improve slightly with increasing electrolyte advection, this merely indicates that the reactant transport through the nano-pore is improving. The M-H device performance does not change significantly with increasing electrolyte advection, as to be expected due to the higher concentration of reactants making transport limitations negligible.

The lack of a flow rate effect in the wider nano-pore device is because the nano-pores are now significantly wider than the EDLs. So the charged regions of the electrolyte no longer extend into the bulk (middle) region of the nano-pore where the advection is present. Therefore, the electrolyte advection flux within the EDL has become negligible and no longer alters the EDL structure. Additionally, the performance of the wider nano-pore devices is significantly less than that of the narrower nano-pore devices for all flow rates.

This is because effective surface area of the electrodes has decreased with the wider pores, as well as the lack of the EDL advection performance enhancement.

Figures 4(a) and 4(b) show the power density performance data for a H-O and M-H device, respectively, where the nano-pore lengths are twice that of the devices presented above ($d_2 = 2\mu\text{m}$) in Figure 2. In these devices, the electrolyte advection induced performance enhancement is even more prevalent than in the shorter nano-pore devices. The peak power density for both H-O and M-H fuel cells is more than double for a device with $V_{Avg} = 20\text{ mm/s}$ than for a device with $V_{Avg} = 2\text{ mm/s}$. This is because in longer nano-pores the electrolyte advection has a greater effect on the EDL structure, offering further performance improvements. In fact, at lengths long enough, very interesting non-linear electrolyte potential and concentration distributions begin to arise along the axis of the nano-pore causing the electrostatic restriction to be eliminated in the upstream regions (not shown). The results in Figure 4 confirm that, through the use of nano-pores, the introduction of an advection flux within the EDL can offer significant performance improvements at the device level by altering the EDL structure in a way that has not been studied before.

It should also be noted that the overall performance for both H-O and M-H fuel cells with longer nano-pores is even greater than that in Figure 2 for all flow rates. This can be attributed to greater electrolyte advection performance improvements as well as increased effective surface area of the electrodes. However, the M-H fuel cell performance is still greater than that of the H-O fuel cell which shows

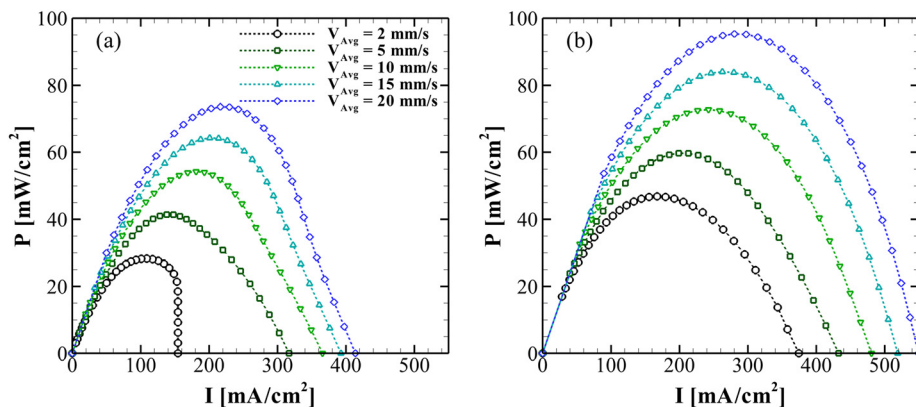


FIG. 4. Power density performance for a (a) H-O and (b) M-H device with twice the nano-pore lengths ($d_2 = 2\mu\text{m}$) and various average electrolyte velocities, V_{Avg} . All other conditions are same as in Figure 2.

evidence of greater reactant transport limitations. This confirms that the nano-pore based device configuration is best suited for direct liquid reactants due to the high susceptibility to reactant transport limitations. Even so, improving electrode kinetics by altering the EDL through nano-patterning is the future of electrode design and electrochemical devices. The performance could potentially be improved even further by nano-pores that are narrower than the Debye length. However, we did not study such conditions as it may not be practically possible to decrease the pore dimensions to that scale.

¹A. A. Franco, P. Schott, C. Jallut, and B. Maschke, *Fuel Cells* **7**(2), 99 (2007).

²I. B. Sprague and P. Dutta, *Numer. Heat Transfer, Part A* **59**(1), 1 (2011).

³P. M. Biesheuvel, M. van Soestbergen, and M. Z. Bazant, *Electrochim. Acta* **54**(21), 4857 (2009).

⁴I. Sprague and P. Dutta, *Electrochim. Acta* **56**(12), 4518 (2011).

⁵K. Aoki, *J. Electroanal. Chem.* **488**(1), 25 (2000).

⁶R. He, S. L. Chen, F. Yang, and B. L. Wu, *J. Phys. Chem. B* **110**(7), 3262 (2006).

⁷J. Lim, J. D. Whitcomb, J. G. Boyd, and J. Varghese, *Comput. Mech.* **43**(4), 461 (2009).

⁸X. Lang, A. Hirata, T. Fujita, and M. Chen, *Nat. Nanotechnol.* **6**, 232 (2011).

⁹T. A. Zangle, A. Mani, and J. G. Santiago, *Chem. Soc. Rev.* **39**(3), 1014 (2010).

¹⁰J. Y. Jung, P. Joshi, L. Petrossian, T. J. Thornton, and J. D. Posner, *Anal. Chem.* **81**(8), 3128 (2009).

¹¹C. Kubeil and A. Bund, *J. Phys. Chem. C* **115**(16), 7866 (2011).

¹²K. S. Salloum and J. D. Posner, *J. Power Sources* **195**(19), 6941 (2010).

¹³I. B. Sprague and P. Dutta, *SIAM J. Appl. Math.* **72**(4), 1149–1168 (2012).